The Astrophysical Journal Letters, 1000:L49 (7pp), 2026 April 1 https://doi.org/10.3847/2041-8213/ae524a

High-resolution Near-Infrared Spectroscopy of the B[e] Supergiant LHA 115-S 18: Discovery of Hot Water Vapor Emission

María Laura Arias[1,2,4], Andrea Fabiana Torres[1,2,4], Michaela Kraus[3], and Lydia Sonia Cidale[1,2,4]
[1] Instituto de Astrofísica La Plata, CCT La Plata, CONICET-UNLP, Paseo del Bosque S/N, 1900, La Plata, Argentina; mlaura@fcaglp.unlp.edu.ar
[2] Facultad de Ciencias Astronómicas y Geofísicas, Universidad Nacional de La Plata, Paseo del Bosque S/N, 1900, La Plata, Argentina
[3] Astronomical Institute, Czech Academy of Sciences, Fričova 298, 251 65 Ondřejov, Czech Republic
Received 2025 December 30; revised 2026 March 13; accepted 2026 March 15; published 2026 March 27

Abstract

The post-main-sequence evolution of massive stars involves phases of intense, often eruptive mass loss, including the B[e] supergiant phase. These hot stars are surrounded by cool, dense circumstellar disks that host complex chemistry, producing both molecules and dust. Understanding the mass-loss history of B[e] supergiants is essential for constraining stellar evolution models, particularly regarding their final stages. Near-infrared CO band emission serves as a key tracer of disk dynamics, typically arising from the inner edge of the molecular disk or ring. However, the oxygen-rich environments of these stars also favor the presence of other molecules that trace regions complementary to those probed by CO. In this work, we present high-resolution near-infrared spectra of the Small Magellanic Cloud B[e] supergiant LHA 115-S 18. Our analysis reveals rotationally broadened CO emission consistent with a Keplerian molecular ring, alongside strong hydrogen wind features in both *H* and *K* bands and numerous metallic emission lines. Notably, we report the first detection of hot water vapor emission in a B[e] supergiant. This finding indicates the existence of extended cool and dense regions in a harsh environment. A radial velocity offset between molecular and Pfund line emission further supports a binary system, with the molecular gas potentially being circumbinary. The discovery of hot H_2O around the B[e] supergiant star LHA 115-S 18 challenges classical models on the evolution and chemistry of massive binary stars and provides critical insight into mass-loss processes and molecular enrichment of the interstellar medium.

Unified Astronomy Thesaurus concepts: Circumstellar matter (241); B supergiant stars (130)

1. Introduction

LHA 115-S 18 is a highly peculiar luminous star located at the Small Magellanic Cloud (SMC). Despite being the subject of numerous studies over the past several decades, its true nature remains controversial. F. J. Zickgraf et al. (1989) classified it as a B[e] supergiant (B[e] SG) and derived its fundamental parameters: $T_{\rm eff} = 25\,000$ K, $\log g = 3.0$, $E(B-V) = 0.4$, $L_* = 3.0\text{-}4.6 \times 10^5\ L_\odot$, $R_* = 33\text{–}36\ R_\odot$, and a zero-age main-sequence (ZAMS) mass of $M \approx 35\text{–}40\ M_\odot$. The star displays significant photometric and spectroscopic variability on different timescales, from days to years, resembling in some aspects a luminous blue variables in its quiescent phase (P. W. Morris et al. 1996; E. S. Bartlett & J. S. Clark 2015). Most notable are the Balmer lines that change from a pure-emission to a P Cygni profile and the line of He II λ4686 that changes from absence of the line to emission with the same strength as Hβ (N. Sanduleak 1977; M. Azzopardi et al. 1981; S. N. Shore et al. 1987). This latter fact, together with the identification of an X-ray counterpart source (J. S. Clark et al. 2013; G. Maravelias et al. 2014) and the presence of Raman-scattered emission lines in the optical range (A. F. Torres et al. 2012), suggests that LHA 115-S 18 is probably a binary system composed by a B SG and a hot compact object. Additionally, molecular emission bands of titanium monoxide (TiO) and carbon monoxide (CO) in the optical and near-infrared spectra of LHA 115-S 18, respectively, were reported (F. J. Zickgraf et al. 1989; P. W. Morris et al. 1996; M. E. Oksala et al. 2013), suggesting the presence of cool, dense molecular gas in the circumstellar environment (P. W. Morris et al. 1996; A. Liermann et al. 2010). CO and TiO bandhead emission also seems to be variable (M. Kraus et al. 2023; A. F. Torres et al. 2012). The star also shows a strong infrared excess due to dust (J. H. Kastner et al. 2010).

The disks of B[e] SGs present appropriate physical conditions to facilitate efficient molecule formation and dust condensation. In such environments, where the number of oxygen atoms is greater than the number of carbon ones (O/C>1), the latter are locked in CO molecules. Due to its high dissociation temperature (∼5000 K), the CO molecule can persist much closer to hot radiation sources than all other molecules, making it an effective tracer of the inner rim of circumstellar molecular rings (M. Kraus et al. 2000). In addition, excess oxygen atoms are available for the formation of other molecules or compounds, such as silicon monoxide (SiO), which has the second highest dissociation energy after that of CO, and TiO. The emission from the SiO band at ∼4 μm was discovered in four Galactic B[e] SGs (M. Kraus et al. 2015), while emission from TiO bands in the optical spectral range was reported for five Magellanic Cloud B[e] SGs (F. J. Zickgraf et al. 1989; A. F. Torres et al. 2012, 2018; M. Kraus et al. 2016). Although these detections have not been the result of a systematic study, they offer a promising avenue for the search for other molecules that could be sensitive tracers of the physical properties of the B[e] SG disk regions

[4] Member of the Carrera de Investigador Científico, CONICET, Argentina.

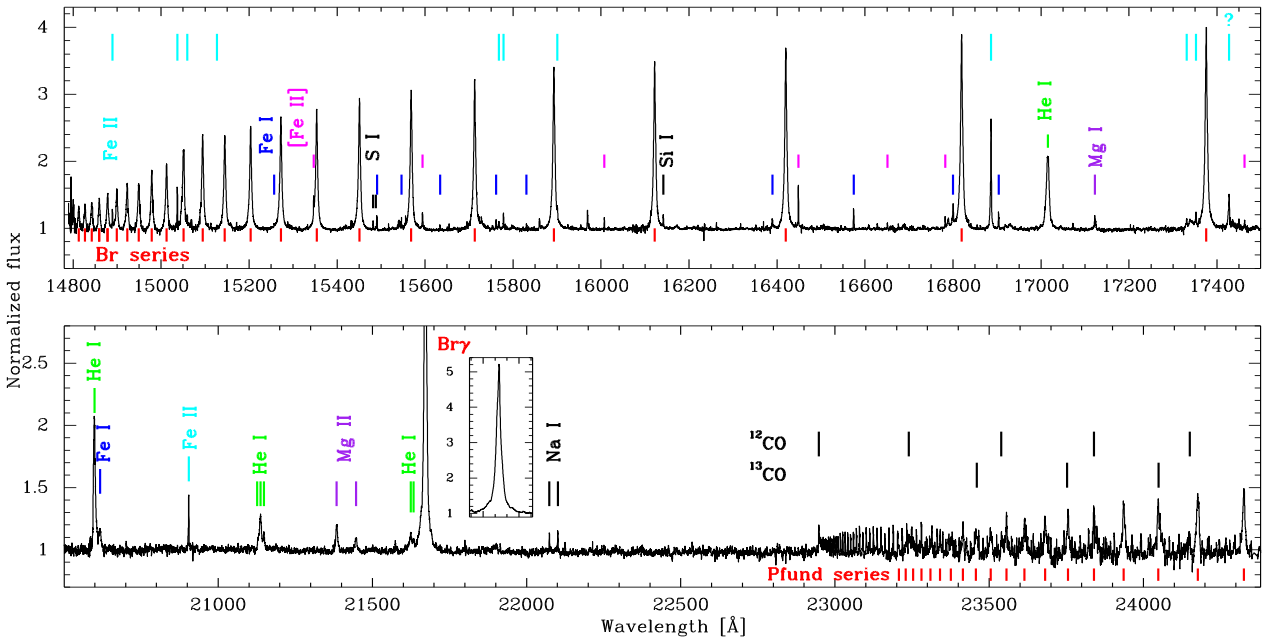

Figure 1. GEMINI/IGRINS *H*-band (top) and *K*-band (bottom) IGRINS high-resolution spectrum of the star LHA 115-S 18. Positions of the CO band heads, Pfund emission lines, and He I lines are marked with ticks and labeled. We also indicate the identified metallic emission lines.

prior to the dust condensation zone. A good candidate for a more complex O-bearing molecule is water (H_2O). Water vapor features have been reported from the environments of evolved late-type stars, such as the extreme C-rich asymptotic giant branch (AGB) star IRC+10216 (G. J. Melnick et al. 2001), the oxygen-rich AGB star W Hydrae (D. A. Neufeld et al. 1996), the red SG VY Canis Majoris (D. A. Neufeld et al. 1999), and the yellow hypergiant HD 269953 (M. Kraus et al. 2022). Most of the water detections cited above are in the infrared region in the *K* band or beyond.

In this work, we report the first detection of hot water vapor in the circumstellar disk of the SMC SG LHA 115-S 18. We present high-resolution near-IR spectroscopic observations of the star and model in detail the H_2O emission spectrum, together with CO molecular emission and Pfund line emission observed in the *K* band.

2. Observations and Data Reduction

LHA 115-S 18 was observed with Immersion GRating INfrared Spectrometer (IGRINS) mounted on the Gemini South telescope, on 2021 October 3 under the program GS-2021B-Q241. The IGRINS spectrograph fully covers the *H* and *K* bands in the near-IR (1.45–2.45 μm) in a single exposure. The slit size is $0\farcs34 \times 5''$, and the resolving power is $R \approx 45{,}000$ (I.-S. Yuk et al. 2010; C. Park et al. 2014; G. Mace et al. 2016). The observations were taken in one ABBA nodding sequence, with an exposure time of 650 s per offset position, obtaining a mean signal-to-noise ratio (S/N) of 80. Data were reduced using the IGRINS Pipeline Package (IGRINS PLP; J.-J. Lee et al. 2017) that performs sky subtraction, flat-fielding, bad-pixel correction, aperture extraction, and wavelength calibration using sky OH emission lines. To eliminate telluric lines, each science spectrum was divided by a telluric standard A0V star spectrum (HIP1714) observed close in time and at a similar air mass to that of the science target. As the strongest telluric features were not completely removed during the data reduction procedure with the IGRINS PLP, we reprocessed this step using the "telluric" task from the IRAF[5] package. Still, some telluric residuals remain mainly as weak absorption features throughout the entire spectral range. A model spectrum of Vega, provided by the IGRINS PLP, was then multiplied by the divided spectra to correct for the intrinsic lines of the standard star, which are mainly H lines. The spectra were corrected for heliocentric velocity.

3. Results

3.1. H- and K-band Atomic Spectrum

In Figure 1, we show the IGRINS high-resolution *H*- and *K*-band spectra of LHA 115-S 18, where we indicate the identification of the strongest lines. Pfund (*K*-band) and Brackett (*H*-band) hydrogen lines appear in emission with one-peaked profiles. Also noticeable are He I emission lines at 1.700, 2.050, 2.112/113, and 2.161 μm, and several Fe I, Fe II, and [Fe II] emission lines. The *K*-band spectrum shows emission lines from Mg II doublet at 2.138/144 μm and Na I doublet at 2.206/209 μm, and a few other lines of neutral atoms. These lines trace the atomic gaseous envelope, revealing a stratified structure. The H I and He I lines and single ionized metallic lines form in a highly ionized inner wind/disk, while Na I lines and other neutral atomic lines in an outer cooler region ($T < 5000$ K) are shielded from the star by the dense inner layers.

3.2. CO Band Emission

CO bands in emission are observed in the *K*-band spectrum of LHA 115-S 18. The high spectral resolution provided by IGRINS allowed us to resolve individual rovibrational lines of CO, in particular shortward of the second ^{12}CO band head.

[5] IRAF is distributed by the Community Science and Data Center at NSF NOIRLab, which is managed by the Association of Universities for Research in Astronomy (AURA) under a cooperative agreement with the U.S. National Science Foundation

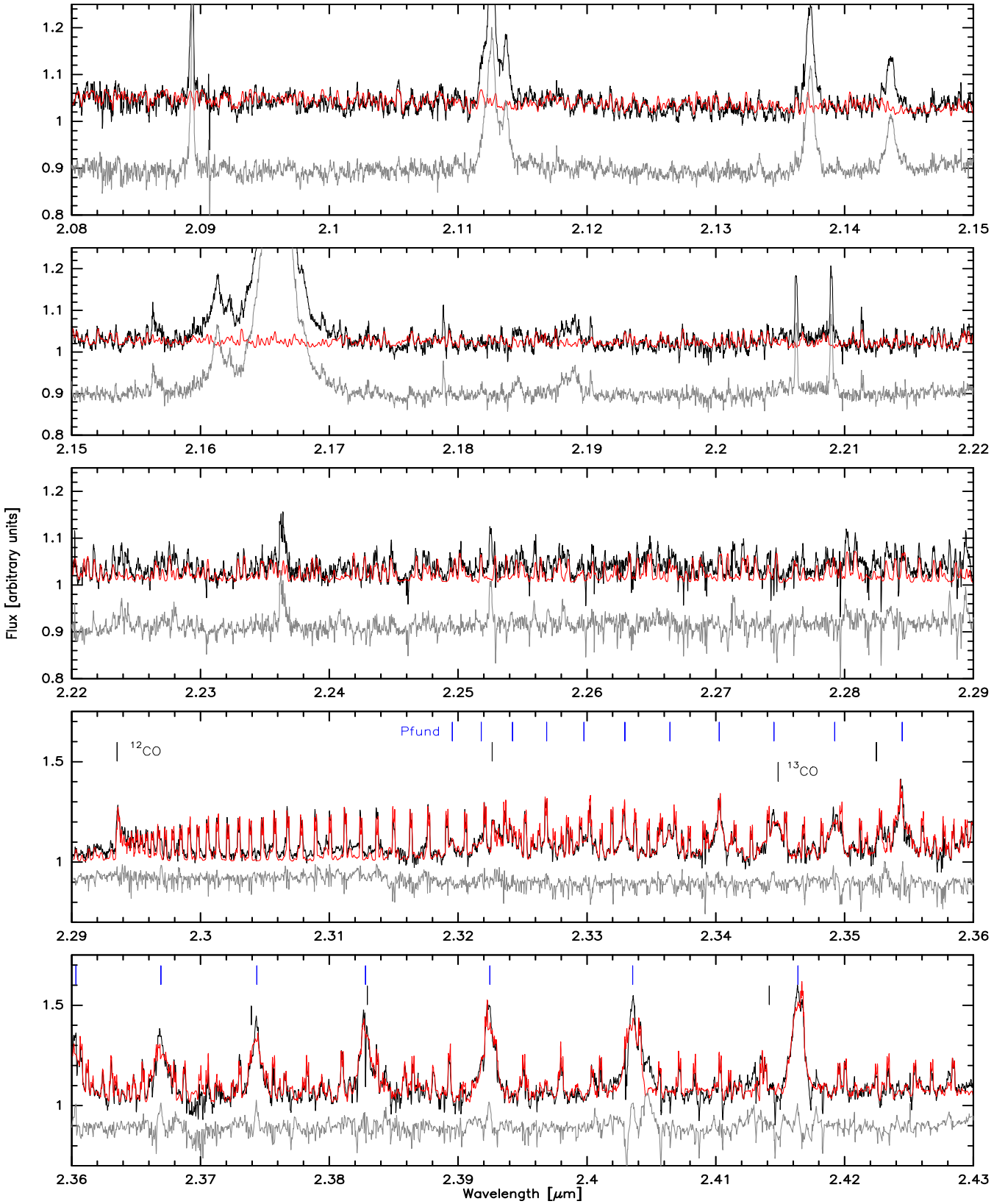

Figure 2. GEMINI/IGRINS observed *K*-band spectrum of LHA 115-S 18 (black), with the model composed of water vapor (red, top three panels) and water vapor + CO bands + Pfund lines (red, bottom two panels) overplotted, along with the residuals shifted for better visibility (gray).

Their profiles appear double-peaked (see Figure 2), suggesting rotation or equatorial in-/outflow of the gas. Based on our experience with CO emission around evolved massive stars, where the line-forming region is usually confined in a narrow ring (e.g., L. S. Cidale et al. 2012; M. F. Muratore et al. 2015; A. F. Torres et al. 2018; M. L. Arias et al. 2021), we adopted

Table 1
Best-fitting Model Parameters

	CO	Water Vapor	Pfund Lines
T (K)	2000 ± 200	1800 ± 200	⋯
N (10^{21} cm^{-2})	0.2 ± 0.05	5 ± 1	⋯
$v_{\rm rot,proj}$ (km s^{-1})	12 ± 0.5	⋯	⋯
$v_{\rm Gauss}$ (km s^{-1})	⋯	10 ± 0.5	⋯
^{12}CO/^{13}CO	5	⋯	⋯
$v_{\rm wind}$ (km s^{-1})	⋯	⋯	80 ± 0.5
T_e (K)	⋯	⋯	10^4
N_e (10^{12} cm^{-3})	⋯	⋯	20

the scenario of a rotating ring of molecular gas for modeling the emission from LHA 115-S 18. We utilized the code developed by M. Kraus et al. (2000) for the computation of ^{12}CO band emission from a circumstellar disk, modified by M. Kraus (2009) and M. E. Oksala et al. (2013) to add the emission of the isotopic molecule ^{13}CO. The model considers that the CO gas is in local thermodynamic equilibrium, which is a suitable approximation for circumstellar environments, given their typical high column densities (M. E. Oksala et al. 2012; M. Kraus et al. 2016, 2020). The *K*-band spectrum of LHA 115-S 18 also contains emission from the molecular isotope ^{13}CO. The detection of measurable amounts of ^{13}C, locked into ^{13}CO molecules, is an unambiguous tracer for chemically enriched material and age of the star (M. Kraus 2009; A. Liermann et al. 2010). We determined a ^{12}CO/^{13}CO isotopic ratio of 5 ± 1. This value mirrors the stellar surface enrichment in ^{12}CO/^{13}CO at the time of mass ejection, indicating that LHA 115-S 18 is an evolved (post-red supergiant) object. Our best-fitting parameters to the CO emission are listed in Table 1.

3.3. Emission from Water Vapor

The *K*-band spectrum of LHA 115-S 18 also displays many small emission features shortward of and within the CO bands, which we identified as lines from water vapor (Figure 2). We computed synthetic spectra for a model similar to that of CO, i.e., considering a ring of gas with constant temperature and column density, and using the line list, energy levels, and Einstein transition coefficients from O. L. Polyansky et al. (2018). This is the most complete line list of water spreading from the UV to the infrared that was computed in the frame of the ExoMol project.[6] We have cropped this list to the wavelength region of interest for our data, and it still contains more than 400 million lines that we have included in our computation of the emission spectrum.

The water vapor lines show no indication for rotational broadening, so we use a Gaussian profile with a velocity of 10 ± 0.5 km s^{-1}, which might be interpreted as turbulent motion of the gas. The best-fitting parameters are listed in Table 1, and the synthetic spectrum of water vapor, which spreads over the full observed wavelength range, is included in the synthetic spectrum shown in red in Figure 2, and is the sole fitting component in the top three panels. In these panels, most of the observed emission features can be identified with emission from water vapor. Also worth mentioning is the fact that the numerous water vapor lines all overlap, forming a quasi-continuum, so that basically no line-free continuum is evident throughout the entire spectrum.

[6] https://www.exomol.com

To show the sensitivity of the model fits to the adopted parameters, we performed a targeted exploration of the H_2O column density and temperature. To keep the computational effort manageable, this analysis was carried out for three representative wavelength intervals (P1, P2, and P3), which are indicated in the top panel of Figure 3. For the temperature, we computed models for T = 1400, 1600, 1800, 2000, and 2200 K while keeping the column density fixed at our best-fit value of N(H_2O) = 5 × 10^{21}cm^{-2}.

The comparison (shown in Figure 3, four top panels) demonstrates that temperatures of 1400 and 2200 K clearly fail to reproduce the observed emission pattern. The best agreement in regions P1 and P2 is obtained for $T \approx 1800$ K, while models with ±200 K already produce noticeable discrepancies in the relative intensity of the emission features. This supports our adopted uncertainty of approximately ±200 K, which we consider a conservative estimate.

For the column density, we computed models for $N(H_2O)$ = 1×10^{21}, 4×10^{21}, 5×10^{21}, 6×10^{21}, and 1×10^{22} cm^{-2} at a fixed temperature of T = 1800 K. As illustrated in Figure 3 (four bottom panels), the lowest column density corresponds to an almost optically thin case and significantly underpredicts the emission strength. In contrast, $N(H_2O) = 1 \times 10^{22}$ cm^{-2} approaches the optically thick limit in region P1. The best agreement is obtained for column densities around $N(H_2O)$ ≈ 4–6 × 10^{21} cm^{-2}, consistent with the value adopted in Table 1.

3.4. Pfund Line Emission

The spectrum of LHA 115-S 18 displays emission from the hydrogen Pfund line series superimposed on the CO band spectrum. These lines show single-peaked profiles, suggesting that they form in a dense ionized wind rather than in a rotating or outflowing disk. This high-density environment can lead to pressure ionization effects, and hence to a sharp cutoff in the maximum number of detectable Pfund lines. Thus, the maximum detectable Pfund line is an indicator of the hydrogen density in the line-forming region. To include the contribution of these lines to the total emission spectrum, we apply the code developed by M. Kraus et al. (2000) for the computation of the hydrogen series according to Menzel case B recombination, assuming that the lines are optically thin (J. H. Kastner et al. 2010). The shape of the Pfund line emission spectrum is not sensitive to the electron temperature. We therefore fix the temperature at T_e = 10,000 K, which is a typical value for an ionized wind. As the line profiles show no indication of rotational broadening, we adopt a pure Gaussian profile, which is a reasonably good approximation for optically thin recombination lines formed in a stellar wind. The maximum detectable Pfund line is Pf 38-5. The parameters of the best-fitting model for the Pfund lines are listed in Table 1. We notice a blueshift of the Pfund lines by about 25 km s^{-1} with respect to the molecular lines.

4. Discussion and Conclusions

We present high-resolution ($R \approx$ 45,000) simultaneous *H*- and *K*-band spectroscopic observations of the B[e] SG LHA 115-S 18, obtained using the IGRINS spectrograph. Our data provide a detailed view of the near-infrared spectrum, dominated by intense wind emission lines from the Brackett and Pfund series and numerous emission lines from metals.

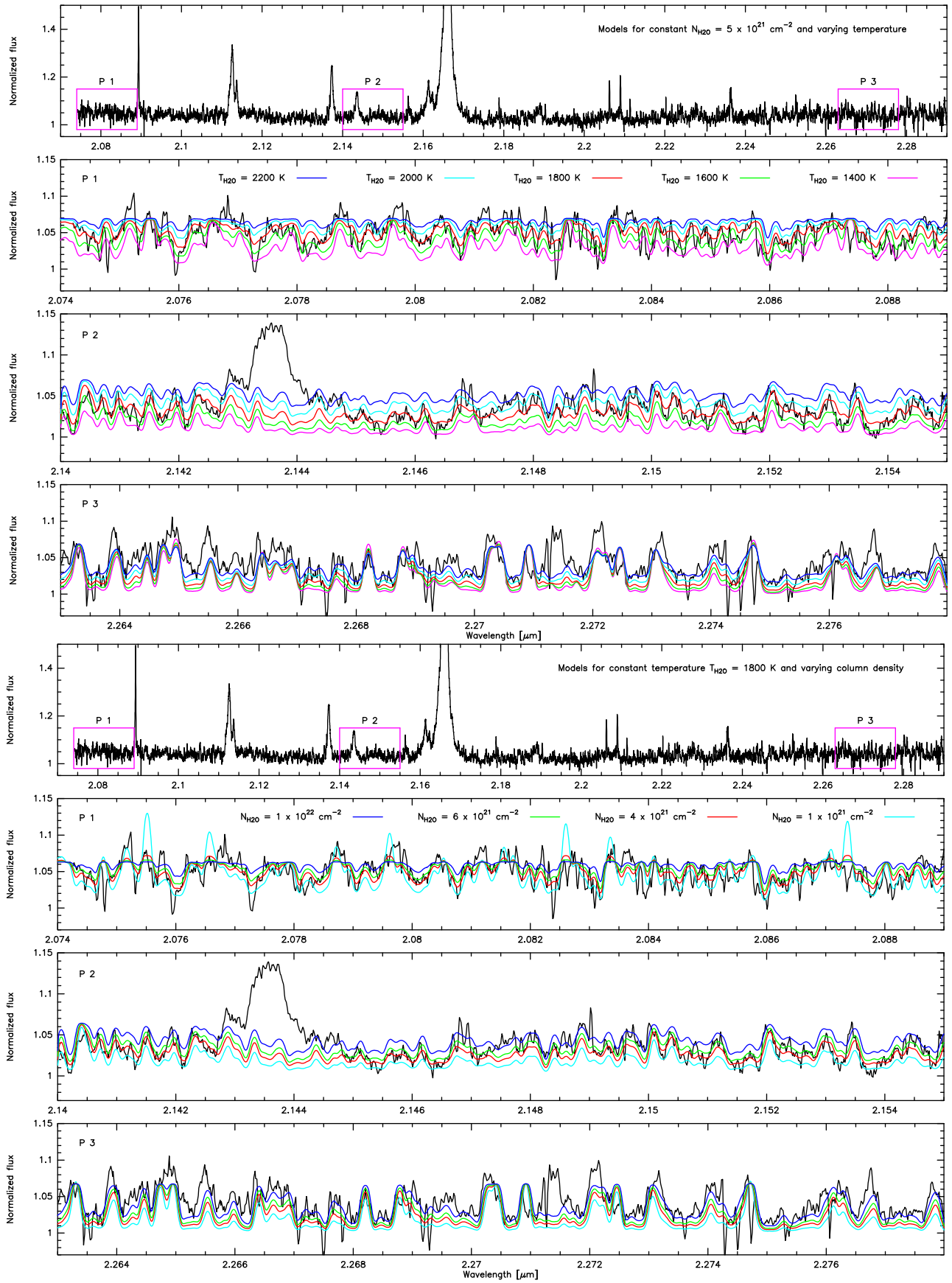

Figure 3. Different fits for selected portions of LHA 115-S 18 *K*-band spectrum, showing the variation with the model parameters: temperature and column density. The best fit is for $T(H_2O) \approx 1800$ K and $N(H_2O) \approx 4$–6×10^{21} cm^{-2}.

Moreover, the high quality of the spectroscopic observations of LHA 115-S 18 allows us to clearly resolve rotationally broadened emission from CO bandheads, consistent with a Keplerian rotating ring of molecular gas, as is typical for this class of stars. By modeling this CO emission, we were able to refine the physical parameters of its emitting region. The main result of this article is the identification of many weak emission features, shortward of and within the CO band emission region (from 2.45 to 2.75 μm), which correspond to hot water vapor.

While water vapor has been reported from the environments of evolved late-type stars, this is, to our knowledge, the first detection of water vapor from a B[e] SG star. Modeling the water vapor emission, we found that the lower temperature and the narrower line profiles—when compared with those of the CO emission—indicate that the line-forming region lies farther away from the star. The measured shift in radial velocity between the molecular and the Pfund line emission seen in our spectrum supports a binary nature of the object. If this is the case, the molecular gas might be either circumstellar around the companion or circumbinary.

We also derive a column density ratio of $N(\mathrm{H2O})/N(\mathrm{CO}) \approx 25$, which is broadly consistent with expectations for the oxygen-rich circumstellar environment typical of B[e] SGs. As, in these environments, $\mathrm{C/O} \ll 1$, most of the available carbon is expected to be locked into CO, and the remaining oxygen can then participate in the formation of other oxygen-bearing molecules, including H_2O. If the emitting area of the H_2O region is larger than that of the CO region, the resulting column density ratio $N(\mathrm{H2O})/N(\mathrm{CO}) \approx 25$ is plausible.

The discovery of water vapor emission in LHA 115-S 18 is so far unique among B[e] SGs. Such an emission requires dense, heavily shielded, cool (1000–3000 K) gas. When considered together with the well-established presence of CO band emission, dust, and other molecular species, the detection of water vapor strongly suggests that the circumstellar/circumbinary disk of LHA 115-S 18 is chemically more akin to mass-loss products of cool evolved stars—such as yellow hypergiants (YHGs) or post–red SG objects—rather than to the outflows typically associated with classical B[e] SGs. A compelling comparison is provided by the YHG HD 269953 in the Small Magellanic Cloud, which has recently been reported to exhibit hot water vapor emission in its *K*-band spectrum, with the H_2O-emitting region located farther from the star than the CO-emitting zone, consistent with a rotating disk geometry (M. Kraus et al. 2022). The observed ^{13}CO enrichment in HD 269953 indicates that the circumstellar material is of stellar origin and was likely expelled during episodes of enhanced mass loss. It has also been suggested as a binary system (M. Kourniotis et al. 2022). LHA 115-S 18 exhibits a dense, strongly shielded molecular environment with an even lower $^{12}\mathrm{CO}/^{13}\mathrm{CO}$ ratio, which may point to a related evolutionary history with a previous YHG phase. However, LHA 115-S 18 is an exceptional representative of the B[e] SG class. In addition to the B[e] phenomenon, it displays large-amplitude spectroscopic and photometric variability, Raman-scattered line emission in tandem with strong variable He II emission in the optical range, and weak but variable X-ray emission. Together, these properties indicate a highly complex circumstellar environment that is likely shaped, or at least strongly influenced, by binary interaction. In this context, a combined scenario can be considered in which material ejected during a cooler evolutionary phase provides the molecular and dusty components of the circumstellar environment, while binary interaction—or a past common-envelope phase—may have contributed to the formation or long-term confinement of a dense, shielded disk. Thus, LHA 115-S 18 represents a key object for advancing our understanding of the late evolutionary stages of massive stars in low-metallicity environments. Continued multiwavelength monitoring of LHA 115-S 18 is therefore crucial for constraining its binary nature, the structure and dynamics of its circumstellar disk, and its potential evolutionary link between SG B[e] stars and other transitional massive-star phases.

Acknowledgments

This work is based on observations obtained at the international Gemini Observatory, a program of NSF NOIRLab, which is managed by the Association of Universities for Research in Astronomy (AURA) under a cooperative agreement with the U.S. National Science Foundation on behalf of the Gemini Observatory partnership: the U.S. National Science Foundation (United States), National Research Council (Canada), Agencia Nacional de Investigación y Desarrollo (Chile), Ministerio de Ciencia, Tecnología e Innovación (Argentina), Ministério da Ciência, Tecnologia, Inovações e Comunicações (Brazil), and Korea Astronomy and Space Science Institute (Republic of Korea). This work also used the Immersion Grating Infrared Spectrometer (IGRINS) that was developed under a collaboration between the University of Texas at Austin and the Korea Astronomy and Space Science Institute (KASI) with the financial support of the US National Science Foundation 27 under grants AST-1229522 and AST-1702267, of the University of Texas at Austin, and of the Korean GMT Project of KASI. This project is cofunded by the European Union (Project 101183150—OCEANS). M.L.A., A.F.T., and L.S.C. acknowledge the financial support from CONICET (PIP 1337) and the Universidad Nacional de La Plata (Programa de Incentivos 11/G192), Argentina, and M.K. from the Czech Science Foundation (GA ČR, grant No. 25-17532S). Thanks to the referee for the useful comments and suggestions.

ORCID iDs

María Laura Arias https://orcid.org/0000-0002-4016-2501
Andrea Fabiana Torres https://orcid.org/0000-0001-8797-7209
Michaela Kraus https://orcid.org/0000-0002-4502-6330
Lydia Sonia Cidale https://orcid.org/0000-0003-2160-7146

References

Arias, M. L., Vallverdú, R., Torres, A. F., & Kraus, M. 2021, BAAA , 62, 104
Azzopardi, M., Breysacher, J., & Muratorio, G. 1981, A&A, 95, 191
Bartlett, E. S., & Clark, J. S. 2015, in SALT Science Conf. 2015 (SSC2015), ed. D. Buckley & A. Schroeder (SISSA), 55
Cidale, L. S., Borges Fernandes, M., Andruchow, I., et al. 2012, A&A, 548, A72
Clark, J. S., Bartlett, E. S., Coe, M. J., et al. 2013, A&A, 560, A10
Kastner, J. H., Buchanan, C., Sahai, R., Forrest, W. J., & Sargent, B. A. 2010, AJ, 139, 1993
Kourniotis, M., Kraus, M., Maryeva, O., Borges Fernandes, M., & Maravelias, G. 2022, MNRAS, 511, 4360
Kraus, M. 2009, A&A, 494, 253

Kraus, M., Arias, M. L., Cidale, L. S., & Torres, A. F. 2020, MNRAS, 493, 4308
Kraus, M., Arias, M. L., Cidale, L. S., Torres, A. F., & Kourniotis, M. 2022, BAAA, 63, 65
Kraus, M., Cidale, L. S., Arias, M. L., et al. 2016, A&A, 593, A112
Kraus, M., Kourniotis, M., Arias, M. L., Torres, A. F., & Nickeler, D. H. 2023, Galax, 11, 76
Kraus, M., Krügel, E., Thum, C., & Geballe, T. R. 2000, A&A, 362, 158
Kraus, M., Oksala, M. E., Cidale, L. S., et al. 2015, ApJL, 800, L20
Lee, J.-J., Gullikson, K., & Kaplan, K. 2017, igrins/plp 2.2.0, v9, Zenodo, doi:10.5281/zenodo.845059
Liermann, A., Kraus, M., Schnurr, O., & Fernandes, M. B. 2010, MNRAS, 408, L6
Mace, G., Kim, H., Jaffe, D. T., et al. 2016, SPIE, 9908, 99080C
Maravelias, G., Zezas, A., Antoniou, V., & Hatzidimitriou, D. 2014, MNRAS, 438, 2005
Melnick, G. J., Neufeld, D. A., Ford, K. E. S., Hollenbach, D. J., & Ashby, M. L. N. 2001, Natur, 412, 160
Morris, P. W., Eenens, P. R. J., Hanson, M. M., Conti, P. S., & Blum, R. D. 1996, ApJ, 470, 597
Muratore, M. F., Kraus, M., Oksala, M. E., et al. 2015, AJ, 149, 13
Neufeld, D. A., Chen, W., Melnick, G. J., et al. 1996, A&A, 315, L237
Neufeld, D. A., Feuchtgruber, H., Harwit, M., & Melnick, G. J. 1999, ApJL, 517, L147
Oksala, M. E., Kraus, M., Arias, M. L., et al. 2012, MNRAS, 426, L56
Oksala, M. E., Kraus, M., Cidale, L. S., Muratore, M. F., & Borges Fernandes, M. 2013, A&A, 558, A17
Park, C., Jaffe, D. T., Yuk, I.-S., et al. 2014, SPIE, 9147, 91471D
Polyansky, O. L., Kyuberis, A. A., Zobov, N. F., et al. 2018, MNRAS, 480, 2597
Sanduleak, N. 1977, IBVS, 1304, 1
Shore, S. N., Sanduleak, N., & Allen, D. A. 1987, A&A, 176, 59
Torres, A. F., Cidale, L. S., Kraus, M., et al. 2018, A&A, 612, A113
Torres, A. F., Kraus, M., Cidale, L. S., et al. 2012, MNRAS, 427, L80
Yuk, I.-S., Jaffe, D. T., Barnes, S., et al. 2010, SPIE, 7735, 77351M
Zickgraf, F. J., Wolf, B., Stahl, O., & Humphreys, R. M. 1989, A&A, 220, 206